

INCIDENTAL AND NONINCIDENTAL CANINE THYROID TUMORS ASSESSED BY MULTIDETECTOR ROW COMPUTED TOMOGRAPHY: A SINGLE-CENTRE CROSS SECTIONAL STUDY IN 4520 DOGS

GIOVANNA BERTOLINI, MICHELE DRIGO, LUCA ANGELONI, MARCO CALDIN

Thyroid nodules are common in dogs and are increasingly likely to be detected with the increased use of advanced imaging modalities. An unsuspected, nonpalpable, asymptomatic lesion, defined as a thyroid incidentaloma, may be discovered on an imaging study unrelated to the thyroid gland. The objective of this single-center cross-sectional study was to assess the prevalence and computed tomography (CT) characteristics of incidental and nonincidental thyroid tumors in a large population of dogs, using prospective recruitment of patients undergoing CT examination for various reasons during the period of 2005–2015. Unilateral or bilateral thyroid masses were detected in 96/4520 dogs (prevalence, 2.12%; 95% confidence interval [CI], 1.70–2.54%). Seventy-nine (82.3%) lesions were malignant and 17 (17.7%) were benign. Masses were discovered incidentally in 34/96 dogs (overall prevalence of incidentaloma, 0.76%; 95% CI, 0.51–1.02), and 24 (70.6%) of these 34 masses were thyroid carcinomas. Among the CT variables assessed, mineralization, vascular invasion, and tissue invasion were detected only in malignant tumors. Intratumoral vascularization was significantly associated with the presence of thyroid malignancy ($P < 0.001$). Although incidental thyroid nodules in dogs are relatively rare, they are often malignant. Findings indicated that the neck should be thoroughly assessed in middle-aged and old patients undergoing body CT for various reasons. Thyroid nodules detected incidentally on CT should be sampled to avoid missing thyroid cancer. © 2017 American College of Veterinary Radiology.

Key words: computed tomography, dog, thyroid carcinoma, thyroid incidentaloma, thyroid mass.

Introduction

THYROID CANCER IS THE MOST COMMON TUMOR OF THE endocrine system in dogs, with carcinomas accounting for about 90% of clinically detected thyroid masses.^{1,2} Ultrasound, scintigraphy, helical computed tomography (CT), and magnetic resonance imaging (MRI) have been used for the diagnosis and characterization of thyroid masses in dogs.^{3–6} When a thyroid lesion is suspected, ultrasound is usually performed in the awake patient to confirm the presence of a nodule or mass, characterize the lesion, and assess the status of the contralateral gland. Ultrasound can accurately guide fine needle aspirates and thyroid lesion biopsies.^{7,8} Recommendations from most recently published studies state that ultrasound is indicated as an initial screening tool, but that MRI or CT should be performed for preoperative diagnosis and staging purposes.^{8,9}

Carcinomas, which are generally larger than adenomas, can be detected easily by palpation during physical examination.^{1,2,8} However, small benign or malignant thyroid lesions may remain unnoticed on physical examination and can be discovered incidentally during unrelated procedures.^{1,3} In humans, a thyroid incidentaloma is defined as an unsuspected, asymptomatic thyroid lesion that is discovered on an imaging study or during an operation unrelated to the thyroid gland. These lesions are detected most commonly by ultrasound, CT, MRI, and positron emission tomography.¹⁰

Preliminary results of research including 1409 dogs, related to the present study, showed a 1.63% prevalence of thyroid incidentalomas.¹¹ A recent ultrasound study revealed a 15% prevalence of incidental thyroid nodules in a population of 91 hypercalcemic dogs.¹² The ultrasound characteristics of incidental thyroid adenomas and adenocarcinomas are similar, preventing the differentiation of benign from malignant lesions.¹²

The primary aims of this study were to (1) determine the prevalence of thyroid masses in a large number of dogs, (2) determine the prevalence of thyroid incidentalomas, and (3) assess associations between CT characteristics and malignant or benign causes of thyroid lesions. Secondary aims

From the Diagnostic and Interventional Radiology, San Marco Veterinary Clinic (Bertolini, Angeloni), and San Marco Veterinary Laboratory (Caldin) via Sorio 114/c, 35141 Padova, Italy, and Dipartimento di Medicina Animale, Produzioni e Salute, Università degli Studi di Padova Scuola di Agraria e Medicina Veterinaria, Italy (Drigo).

Address correspondence and reprint requests to Giovanna Bertolini, at the above address. E-mail: bertolini@sanmarcovet.it

Received April 19, 2016; accepted for publication November 28, 2016.
doi: 10.1111/vru.12477

Vet Radiol Ultrasound, Vol. 58, No. 3, 2017, pp 304–314.

were to (1) evaluate the epidemiological characteristics of dogs with thyroid tumors and (2) identify possible associations between epidemiological characteristics and thyroid tumors in dogs.

Material and Methods

Study Design, Sample, and Setting

This prospective, cross-sectional study was carried out from May 18, 2005 to April 29, 2015 at the Diagnostic and Interventional Radiology Division of the San Marco Veterinary Clinic. The study population included client-owned dogs that underwent multidetector row computed tomography (MDCT) examination for various reasons, with the owners' permission. Eligibility criteria were (1) inclusion of the thyroid region in the scans, (2) availability of complete precontrast and postcontrast MDCT scans of the neck, (3) performance of whole-body MDCT examination for staging, (4) sampling of thyroid masses for cytopathological and/or histopathological examination and establishment of a final pathology diagnosis, and (5) examination or removal of enlarged lymph nodes seen on MDCT examination (aspiration for cytology or excision with the tumor), with establishment of a final histopathology diagnosis, for patients that underwent thyroidectomy or necropsy. Dogs with clinical records of previous thyroid or parathyroid surgery were excluded from the study. For dogs that underwent repeat imaging after the establishment of an initial MDCT-based diagnosis of a thyroid lesion, only the first examination was used.

Data on patients' histories, physical examination findings, clinicopathological and pathological results, medical therapies administered, surgical and interventional procedures performed, and follow-up assessments were registered in the same database and were available for this study.

Multidetector Row CT Techniques

Multidetector row CT examinations were performed using a 16-MDCT scanner (Lightspeed 16, GE Medical Systems, Milan, Italy) or a second-generation dual-source computed tomography (128-DSCT) scanner (Somatom Definition Flash, Siemens, Erlangen, Germany). All dogs were positioned in sternal recumbency on the CT table. Scanning parameters for 16-MDCT were as follows: helical modality, detector configuration 16×1.25 mm, pitch 0.562:1, and 0.7 s rotation time. Dose parameters were 120 kV and 160–200 mAs, depending on the dog's size. All images were reconstructed using a standard algorithm (nonenhancing–nonsmoothing reconstruction algorithm) with a 512^2 matrix size and 50% overlap section thickness. Dual-source CT examinations were performed with the following settings: one tube, 120 kVp, 400 mAs/rot

(0.28 s), collimation 128×0.6 mm, and increment 0.3 mm; images were reconstructed using a soft-tissue algorithm.

An iodinated, nonionic, iso-osmolar contrast medium (Visipaque, 320 mgI/ml; GE Healthcare, Milan, Italy) was injected at 37°C into a cephalic vein (640 mgI/kg) through a catheter in a uniphasic manner at a rate of 1.5–4 ml/s, followed by a saline flush with same injection rate via a dual-syringe injector system (Medrad, Stellant CT Injection System, Bayer, Milan, Italy). In patients with known thyroid masses that had undergone CT examination for preoperative planning and staging, angiographic studies of the neck were performed using the bolus tracking technique with both scanners (16-MDCT and 128-DSCT). In most other untargeted studies, contrast-enhanced series included a mixed vascular phase of neck imaging. Images were sent automatically to the picture archive and communication system (PACS) and to image analysis workstations.

Image Analyses

In all affected dogs, characteristics of nodules and masses were assessed at the time of CT reporting. The CT report database program (POA System 9.0, version 153; ©1993–2016) requires radiologists to enter keywords when reporting each case. For this study, the database was searched using keywords “thyroid mass,” “thyroid nodule,” and/or “thyroid incidentaloma.” For image analyses, window settings were adjusted to obtain the best visual estimation of the thyroid lobes and surrounding structures. Transverse source images and a combination of two-dimensional multiplanar reformatting and three-dimensional volume rendering postprocessing techniques were used as part of routine assessment of MDCT volume data.

Two authors (G.B., L.A.) evaluated the following characteristics and recorded findings by consensus in a dedicated section of each report: (1) incidental/nonincidental; (2) unilateral/bilateral (masses expanding across the isthmus or hyoid region were considered to be bilateral); (3) side (left/right); (4) size (volume); (5) shape and

TABLE 1. Predominant Breeds, in Order of Frequency, for the Total Population of Sampled Dogs

Breed*	Affected dogs [n (%)]	Unaffected dogs [n (%)]	Total [n (%)]
Mixed breed	31 (32.3)	1305 (29.5)	1336 (29.6)
Labrador Retriever	7 (7.3)	242 (5.5)	249 (5.5)
German Shepherd	3 (3.1)	234 (5.3)	237 (5.2)
Boxer	7 (7.3)	209 (4.7)	216 (4.8)
Golden Retriever	4 (4.2)	138 (3.1)	142 (3.1)
Beagle	6 (6.3)	104 (2.4)	110 (2.4)
Other Breeds	46 (47.9)	2184 (49.3)	2230 (49.4)
Total	96 (2.1)	4424 (97.9)	4520 (100)

*The level of significance for these frequencies comparisons was set after Bonferroni correction for $P < 0.01$.

TABLE 2. Comparisons between Characteristics of the Affected and Unaffected Dogs

Variable		Affected dogs	Unaffected dogs	Total	Significance
Gender [n (%)]	Male	55 (57.3)	2255 (51.0)	2310 (51.1)	<i>P</i> = 0.256
	Female	41 (42.7)	2169 (49.0)	2210 (48.9)	
Sexual status [n (%)]	Castrated	52 (54.2)	2001 (45.2)	2053 (45.4)	<i>P</i> = 0.097
	Intact	44 (45.8)	2423 (54.8)	2467 (54.6)	
Age [$\mu \pm$ SD]		125.3 \pm 26.3	100.4 \pm 44.5	101.0 \pm 44.3	<i>P</i> < 0.001
Body weight [$\mu \pm$ SD]		24.0 \pm 13.7	21.7 \pm 14.7	21.7 \pm 14.7	<i>P</i> = 0.130
Total [n (%)]		96 (2.1)	4424 (97.9)	4520 (100)	

Value in bold refers to statistically significant difference. For further explanation, see the text.

TABLE 3. Comparisons between Characteristics of Dogs with Incidental and Nonincidental Thyroid Mass

Variable		Incidental mass	Nonincidental mass	Total	Significance
Gender [n (%)]	Male	17 (50.0)	38 (61.3)	55 (57.3)	<i>P</i> = 0.390
	Female	17 (50.0)	24 (38.7)	41 (42.7)	
Sexual status [n (%)]	Castrated	22 (64.7)	30 (48.4)	52 (54.2)	<i>P</i> = 0.140
	Intact	12 (35.3)	32 (51.6)	44 (45.8)	
Age [$\mu \pm$ SD]		132.3 \pm 27.8	121.4 \pm 24.9		<i>P</i> = 0.052
Body weight [$\mu \pm$ SD]		23.6 \pm 12.7	24.02 \pm 12.7		<i>P</i> = 0.988
Total [n (%)]		34 (35.4)	62 (64.6)	96 (100)	

TABLE 4. Comparisons between Characteristics of Dogs with Benign and Malignant Thyroid Mass

Variable		Benign	Malignant	Total	Significance
Gender [n (%)]	Male	10 (58.8)	45 (57.0)	55 (57.3)	<i>P</i> = 1.000
	Female	7 (41.2)	34 (43.0)	41 (42.7)	
Sexual status [n (%)]	Castrated	12 (70.6)	40 (50.6)	52 (54.2)	<i>P</i> = 0.180
	Intact	5 (29.4)	39 (49.4)	44 (45.8)	
Age [$\mu \pm$ SD]		128.8 \pm 29.5	124.5 \pm 25.7		<i>P</i> = 0.583
Body weight [$\mu \pm$ SD]		29.5 \pm 12.8	22.8 \pm 13.6		<i>P</i> = 0.064
Total [n (%)]		17 (17.7)	79 (82.3)	96 (100)	

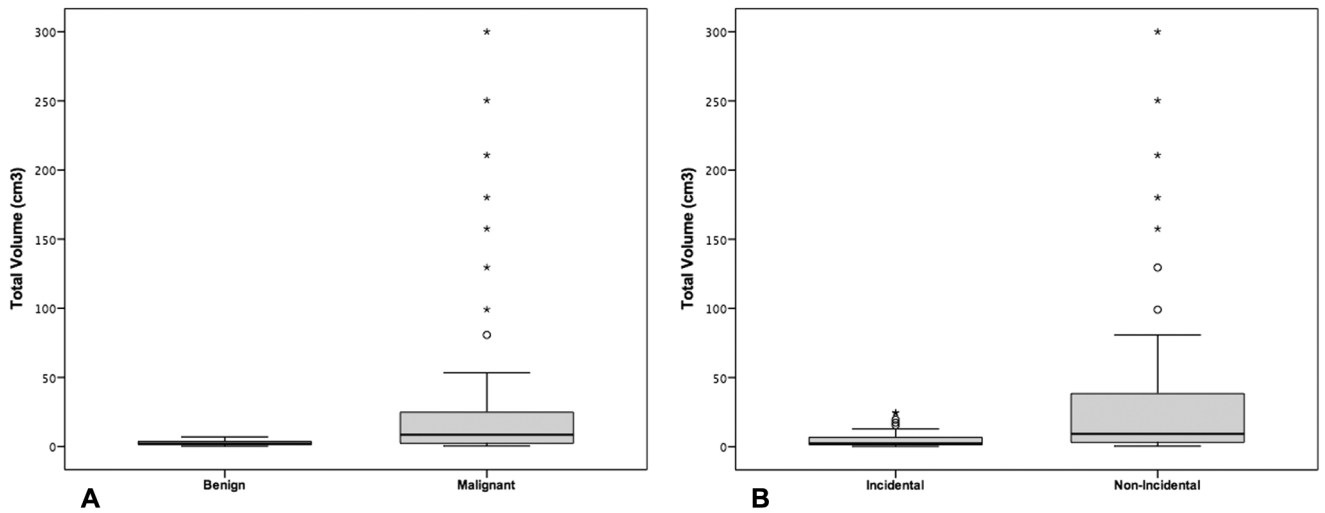


FIG. 1. (A) The graph shows the relationship between volume and the nature of the mass. Larger masses are more likely malignant. (B) Comparison between volumes of incidental and nonincidental thyroid tumors.

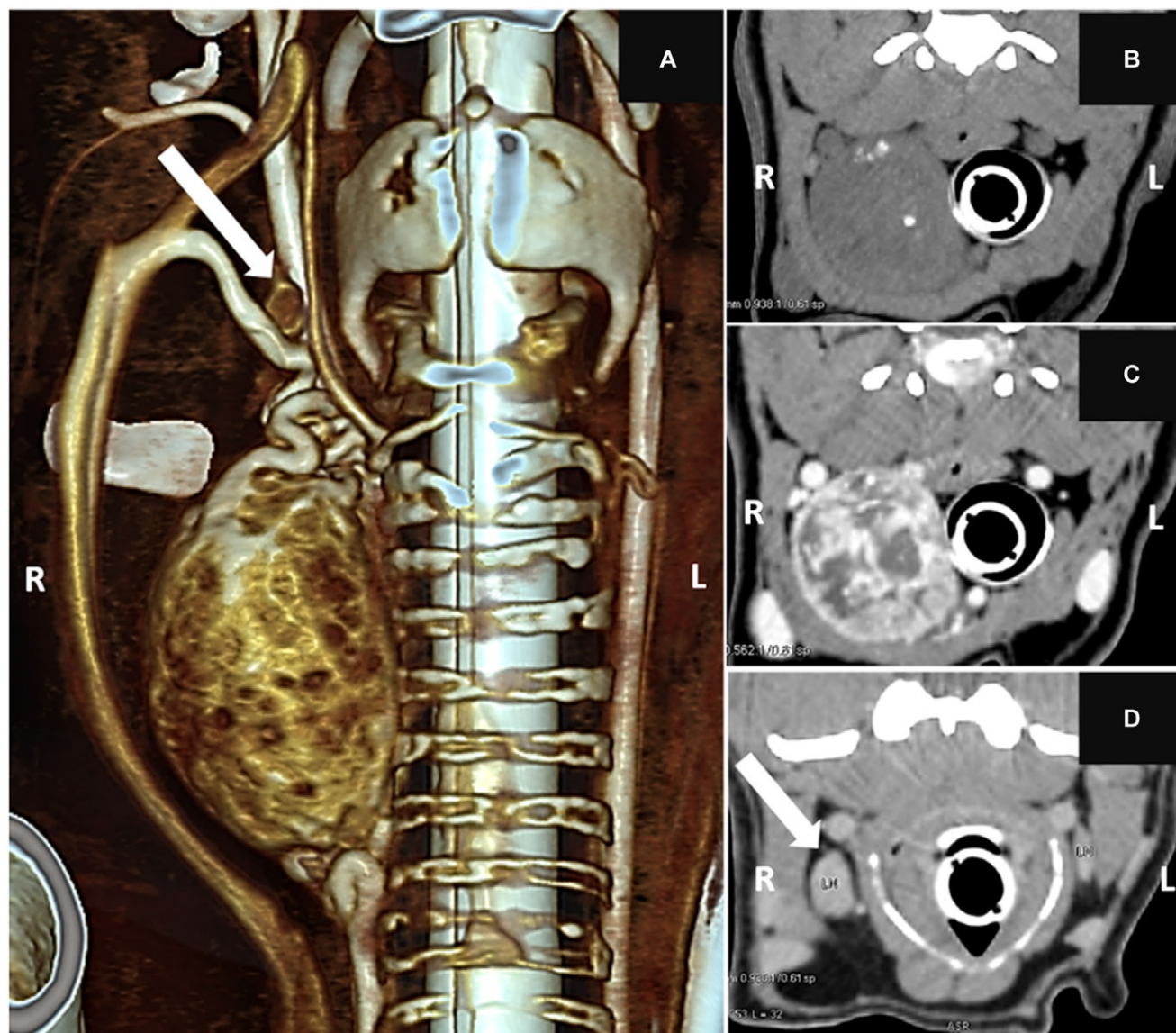


FIG. 2. Targeted MDCT scans of the neck in a 9-year-old, intact female, Beagle dog with known (nonincidental) thyroid carcinoma underwent CT examination for further characterization and staging. (A) Three-dimensional (3D) volume rendered image, ventral view, showing a large ovoid-to-round mass with regular margins of the right thyroid lobe. The white arrow indicates an ipsilateral lymph node metastasis. (B) Precontrast two-dimensional (2D) transverse view. Note the mineralization within the thyroid mass. (C) Postcontrast image of the mass showing multiple small intratumoral vessels enhancing during the angiographic CT series. (D) Two-dimensional transverse view showing an enlarged right medial retropharyngeal lymph node in comparison with the contralateral node. [Color figure can be viewed at wileyonlinelibrary.com]

margins: nodular (when one or more nodules arose within an otherwise normal thyroid gland), ovoid (in case of ovoid-to-round masses with regular margins), and irregularly shaped (ovoid-to-round masses with irregular or ill-defined margins); (6) homogeneity (evaluated subjectively on precontrast scans); (7) presence/absence of mineralization; (8) visual assessment of intratumoral vascularization (small tubular enhancing structures within the tumoral parenchyma; yes/no); (9) qualitative analysis of patterns of parenchymal enhancement of the tumor (homogenous, inhomogeneous, null, peripheral); (10) invasion

of surrounding vascular structures, such as the thyroid veins, internal and external jugular veins, and common carotid arteries (by identification of a mass-like void of contrast medium within the vessel during the angiographic phase of the CT study)¹³; (11) suspected surrounding tissue invasion (lack of distinction between the primary tumor and neighboring tissues, such as the cervical muscles and larynx, esophagus, trachea wall, or obvious luminal invasion of the latter); (12) regional lymph node enlargement, evaluated subjectively or in comparison with the contralateral nodes (mandibular, medial retropharyngeal,

and superficial cervical); and (13) suspected distant metastases (e.g. lung nodules, mediastinal lymph nodes).

The volume of each thyroid lobe was assessed (G.B. and L.A. by consensus) separately using semiautomatic software techniques (Volume Viewer[®], GE Medical Systems or Syngovia, Siemens). Transverse views from reformatted images were selected to measure the volume of the thyroid gland, and lobe contour was outlined precisely on each 1.2/0.6 mm slice. The software calculated the total gland volume by summing the volumes estimated from the areas of all slices. Alternatively, thyroid gland volume was assessed using automated software based on the Response Evaluation Criteria in Solid Tumors (RECIST 1.1).¹⁴

Statistical Methods

Data analyses were selected and performed by two authors (M.D. and M.C.) using the SPSS statistical software package (version 21.0 for Windows; IBM Corporation, Armonk, NY). Data from dogs with and without thyroid masses were compared to identify differences in sex, sexual status, and breed using the chi-squared test with Yate's correction and Fisher's test, as appropriate. The Student's *t* test was used to analyze differences in age and body weight between these groups. Multidetector row CT characteristics were compared between dogs with known thyroid masses and those with thyroid incidentalomas, and between benign and malignant masses, using the chi-squared test with Yate's correction and Fisher's test, as appropriate. The difference in thyroid mass volume between benign and

malignant masses was analyzed using the nonparametric Mann–Whitney *U* test. Values of $P < 0.05$ were considered to be significant.

Results

Characteristics of Dogs Included in the Study

The final population totally comprised 4520 dogs, 96 of which had unilateral or bilateral thyroid tumors (affected dogs) (prevalence, 2.12%; 95% confidence interval [CI], 1.70–2.54%). The comparison group consisted of the remaining 4424 dogs in which no thyroid mass or nodule was identified at the time of CT examination (unaffected dogs). Of the 4520 dogs, which represented 152 breeds, 2310 (51.1%) were male and 2210 (48.9%) were female, with no significant difference in sex ($P = 0.256$) or sexual status ($P = 0.097$). There was no association between breed and thyroid tumor (Table 1). Dogs with thyroid masses were significantly older than dogs in the unaffected group (125.3 ± 26.3 vs. 100.4 ± 44.5 months; $t = 8.97$, $P < 0.001$). Body weight did not differ between the affected and unaffected groups (24.0 ± 13.7 and 21.7 ± 14.7 kg; $t = 1.51$, $P = 0.13$). Characteristics of the two groups are summarized in Tables 2–4.

Computed Tomography Characteristics of Incidental and Nonincidental Thyroid Lesions

Cytopathological results were available for all thyroid masses, and histopathological results were available in most cases (63/96). These results were categorized broadly as

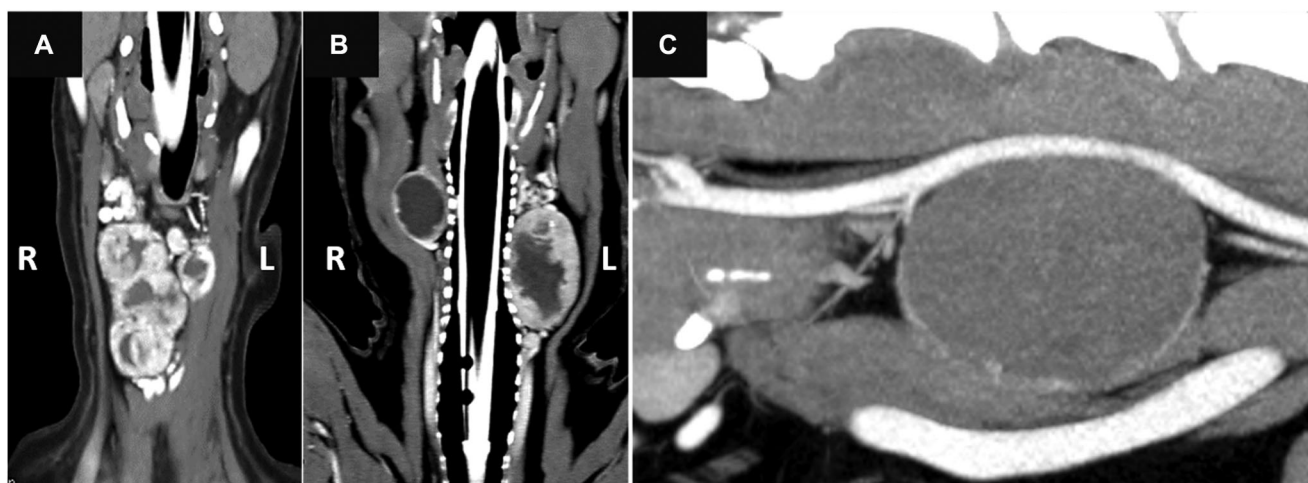


FIG. 3. Patterns of enhancement in three different dogs underwent MDCT examination. (A) Targeted MDCT scan of a nonincidental bilateral, thyroid carcinoma. Note the inhomogeneous pattern of enhancement, with similar characteristics in both thyroid lobes. (B) Bilateral incidental thyroid carcinoma (nontargeted MDCT scan). The left thyroid lobe showed an inhomogeneous pattern, similar to that shown in (A). The mass of the right thyroid lobe had a peripheral enhancement and a large homogeneous, nonenhancing central area. (C) Targeted MDCT scan of a dog with nonincidental unilateral thyroid adenoma. Note the scarce-null enhancement of the mass after contrast medium injection, showing a thin peripheral enhancement.

indicating benign and malignant lesions for this study. Of the 96 affected dogs, 79 (82.3%) had malignant and 17 (17.7%) had benign lesions. Masses were discovered incidentally in 34 of these dogs (overall incidentaloma prevalence, 0.76% [34/4458]; 95% CI, 0.51–1.02), and 24 (70.6%) of these lesions were thyroid carcinomas. In total, almost one-third (24/79) of malignant masses was found

incidentally. Most (83.3%) bilateral masses (18/96 lesions) were malignant and unilateral masses showed similar frequencies of malignancy (right = 81.1% and left = 82.9%). Accordingly, there was no association between the site of the mass and its nature ($P = 0.97$). Most (82%) malignant masses were ovoid-to-round with regular margins while irregular or ill-defined margins were associated only with

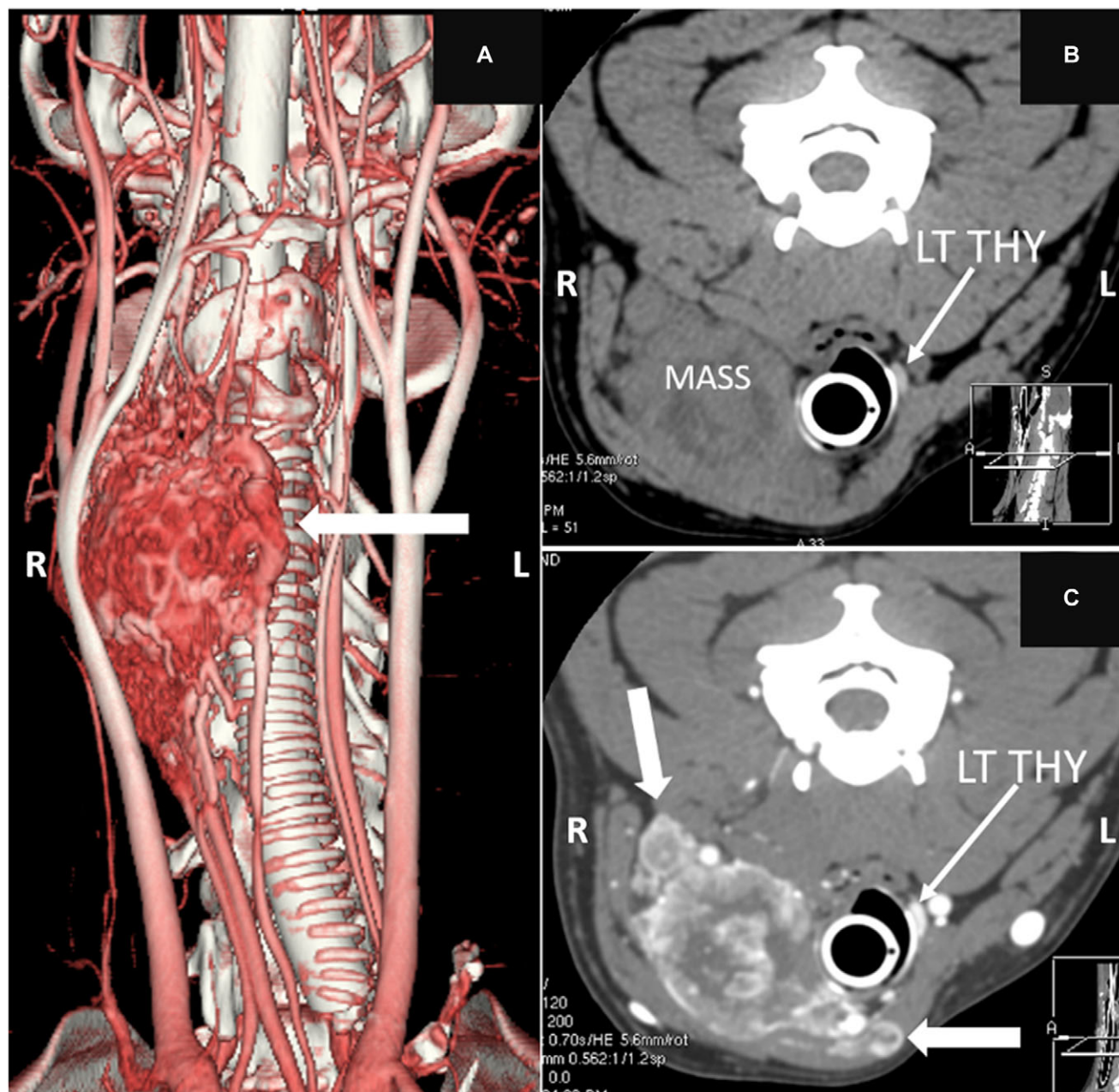


FIG. 4. Targeted MDCT scan of the neck in a dog with nonincidental thyroid carcinoma. (A) Three-dimensional volume rendered image (ventral view) showing the ovoid-to-round, right sided thyroid mass with irregular margins and its relationships with the surrounding vascular structures (arrow). (B) Two-dimensional transverse view of the mass in precontrast scan showing its inhomogenous appearance. The left thyroid lobe had normal appearance (LT THY). (C) Two-dimensional transverse postcontrast image of the same dog, showing the tumoral vascular invasion (arrows). [Color figure can be viewed at wileyonlinelibrary.com]

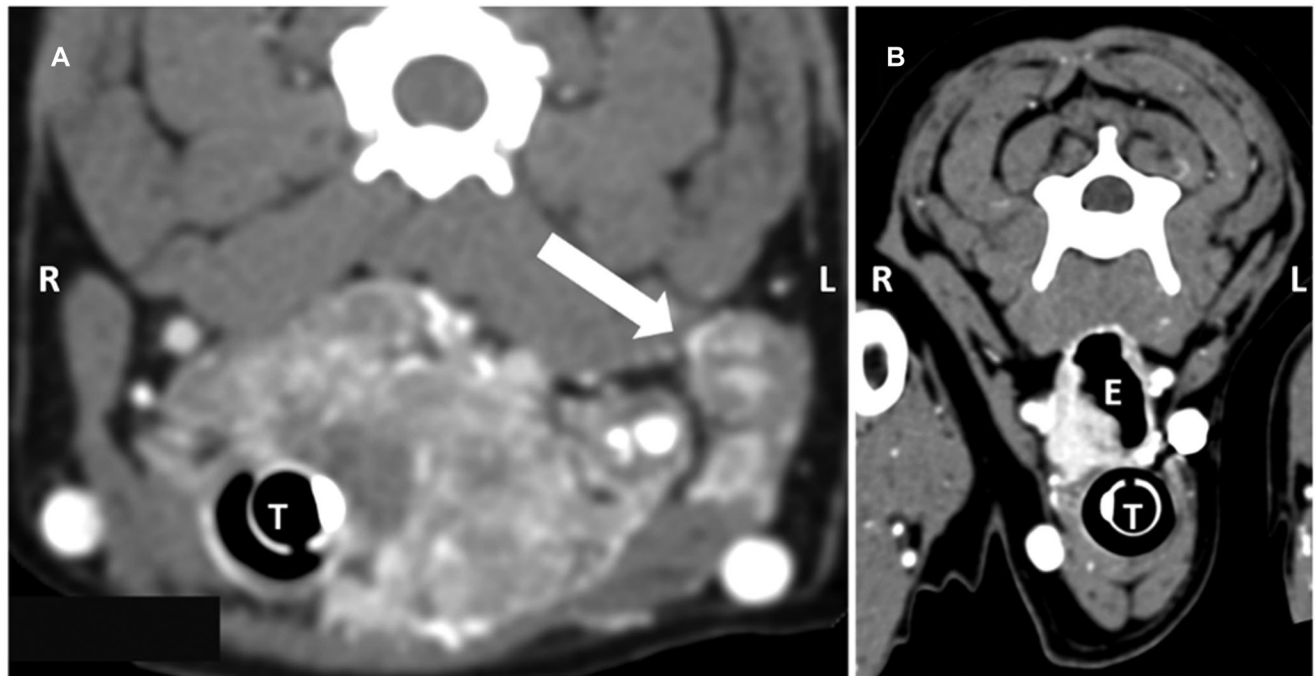


FIG. 5. Transverse CT images from two different dogs with invasive thyroid carcinomas. (A) Two-dimensional transverse view from targeted MDCT scan of the neck in a 10-year-old, female, Mongrel dog, with left sided thyroid carcinoma. The mass was ovoid-to-round with irregular and ill-defined margins showing possible invasion of the tracheal wall and invasion of the surrounding cervical muscles (arrow). (B) Two-dimensional transverse view of the neck in a 9-year-old, female, Golden Retriever with right-sided thyroid mass (not visible here) involving the esophageal wall and projecting into the esophageal lumen. In both cases, necropsy and histopathology confirmed the tissue invasion. E, esophagus; T, trachea.

malignancy. Malignant masses (median, 8.52 cm³; range, 0.42–300 cm³) were significantly larger than benign masses (median, 2.13 cm³; range, 0.29–7 cm³; $U = 298.00$; $P < 0.001$), among known and incidentally discovered lesions ($U = 572.00$; $P < 0.001$; Fig. 1A and B). Areas of mineralization were observed only in malignant masses (Fig. 2). Malignant masses appeared inhomogeneous on precontrast and postcontrast series ($P < 0.001$; Fig. 3). Among the variables intratumoral vascularization, vascular invasion, and tissue invasion, only intratumoral vascularization was associated significantly with the presence of thyroid malignancy, but all were observed only in malignant tumors (Figs. 4 and 5). Lymph node enlargement was associated mostly with malignancy (35 of 37, 94.6%; $P = 0.013$; Table 3; Fig. 6) Distant metastasis (lung nodules) was rare (4/96) and was related exclusively to thyroid malignancy. Computed tomography characteristics of benign and malignant, nonincidental and incidental thyroid masses are summarized in Appendices 1 and 2.

Discussion

In agreement with previous studies,^{1,2} dogs with thyroid tumors in this study were significantly older than unaffected

dogs. Sex and sexual status were not identified as significant risk factors for thyroid tumor development. To the authors' knowledge, this study is the first to test these associations. A variety of trends in breed predispositions to thyroid tumors has been reported in the veterinary literature, but most studies did not account for breed distribution.^{1,15} In a multicentric study, Golden Retrievers, Beagles, and Siberian Huskies were overrepresented.² In the present single-center cross-sectional study, Labradors, golden retrievers, German shepherds, boxers, and beagles were overrepresented, but an association with thyroid tumor development was not identified for any of these breeds.

The CT characteristics described here are similar to those reported for 19 masses in a recent descriptive paper.⁹ In that study, adenomas and carcinomas had very similar appearances, including mineralization, but adenoma volumes were smaller.⁹ There was a considerable overlap between the appearance of benign and malignant thyroid lesions also in the present study. However, some CT features (such as mineralization, irregular shape, intratumoral vascularization, vascular and tissue invasion, and distant metastasis) were found to be related only to malignancy. Malignant masses were significantly larger than benign masses in known and incidentally discovered lesions. Higher mean tumor volumes (57.4 and 65 cm³), about 50 times the normal thyroid

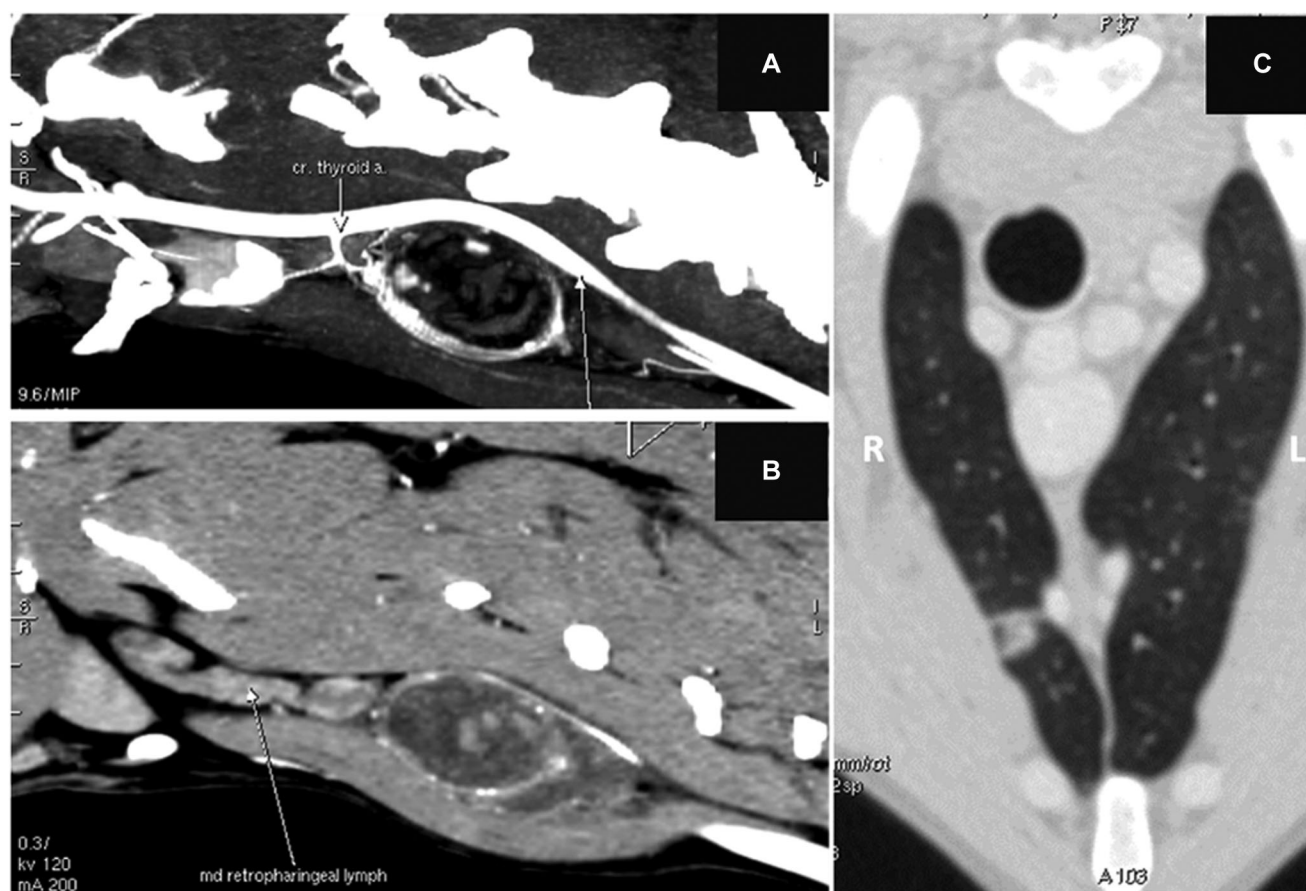


FIG. 6. Metastatic incidental thyroid carcinoma in a 7-year-old, male Boxer dog. (A) Right parasagittal thin-slab maximum intensity projection (MIP) of the neck (cranial is on the left), showing an ovoid-to-round masses with regular margins showing peripheral enhancement in postcontrast series (targeted MDCT scan). (B) Right-parasagittal 2D view, showing the enlarged medial retropharyngeal lymph nodes, just cranial to the mass. (C) Two-dimensional transverse view of the thorax. Note a small ground-glass nodule in the apical right lobe. Postmortem histopathology of the lymph nodes and the small lung nodule confirmed the metastatic nature of these lesions.

volume, have been reported in previous studies.^{8,9} These discrepant results may reflect the inclusion of only large palpable masses in the two previous studies, or the use of an inappropriate measure of central tendency or an error in the unit of measurement.

Benign lesions in affected dogs were generally unilateral, nodular, or ovoid-to-round masses with regular margins, and homogeneous appearance on precontrast scans. Some showed inhomogeneous parenchymal contrast enhancement, but none showed intratumoral vascularization. A possible explanation for these findings is that incidental thyroid nodules were often discovered during nontargeted whole-body CT examinations, which may be suboptimal for the assessment of the intratumoral vascularization. This is a major limitation of the present work. The nature of the mass (lack of intratumoral vascularization) and the level of contrast medium in tissues at the time of image acquisition may explain the contrast enhancement pattern observed in these cases. Again, over the 10-year period of

this study, nonuniform techniques have been used for tumor volume assessment, due to advancement in software technology. This may have introduced some differences in absolute measurements of tumor volumes.

In a recent ultrasound study including 91 hypercalcemic dogs, the prevalence of incidental thyroid nodules was 15%.¹² In that sample, most nodules discovered incidentally were benign (thyroid cyst, nodular hyperplasia, adenoma); 22% were malignant (adenocarcinoma). In the current study, 35% of thyroid tumors were discovered incidentally and 70.6% of them were carcinomas. Almost one-third of malignant masses in affected dogs were found incidentally. A possible explanation for these differences in results is that hypercalcemic dogs represent a subset of the canine population. This discrepancy in frequencies may also reflect geographic factors, such as regional differences in the occurrence of thyroid cancer.

Cytopathological diagnoses were established for all thyroid lesions in this study, whereas histopathological

diagnoses were not available in all cases. This situation represents a potential limitation of the present study. In humans, fine-needle cytology is to be considered highly accurate and cost effective for the assessment of thyroid lesions because it can distinguish between benign and malignant masses.¹⁶ In the veterinary literature, fine-needle cytology is often discounted as being unrewarding and of limited value for the diagnosis of canine thyroid carcinoma,¹⁷ although studies of dogs with thyroid carcinoma have shown close agreement between cytological and histopathological findings.^{18,19}

In conclusion, although incidental thyroid nodules were relatively rare in the dogs included in this study, 70.6% of them were found to be malignant. Based on these results, the neck should be thoroughly assessed in middle-aged and old patients undergoing body CT for other reasons. Further workup would be justified for canine patients with incidental thyroid nodules, especially those exhibiting CT characteristics such as mineralization, irregular shape, in-

tratumoral vascularization, vascular and tissue invasion, and distant metastasis.

LIST OF AUTHOR CONTRIBUTIONS

Category 1

- (a) Conception and Design: Giovanna Bertolini, Marco Caldin, Michele Drigo
- (b) Acquisition of Data: Giovanna Bertolini, Luca Angeloni
- (c) Analysis and Interpretation of Data: Giovanna Bertolini, Marco Caldin, Michele Drigo

Category 2

- (a) Drafting the Article: Giovanna Bertolini
- (b) Revising Article for Intellectual Content: Giovanna Bertolini, Michele Drigo, Marco Caldin

Category 3

- (a) Final Approval of the Completed Article: Giovanna Bertolini, Luca Angeloni, Michele Drigo, Marco Caldin

Appendix 1: The Table Resumes the MDCT Variables Assessed and the Possible Association with the Nature of the Mass (Benign vs. Malignant Lesions)

MDCT feature	Thyroid mass		Total <i>n</i> (%) ^a	Significance
	Benign <i>n</i> (%) ^a	Malignant <i>n</i> (%) ^a		
Site				
Bilateral	3 (17.6)	15 (19.0)	18 (18.8)	<i>P</i> = 0.970
Right	7 (41.2)	30 (38.0)	37 (38.5)	
Left	7 (41.2)	34 (43.0)	41 (42.7)	
Shape				
Irregular	0 (0)	19 (24.1)	19 (19.8)	<i>P</i> = 0.015
Nodular	6 (35.3)	10 (12.7)	16 (16.7)	
Ovoid	11 (64.7)	50 (63.3)	61 (63.5)	
Appearance				
Homogeneous	11 (64.7)	17 (21.5)	28 (29.2)	<i>P</i> < 0.001
Inhomogeneous	6 (35.3)	62 (78.5)	68 (70.8)	
Mineralization				
No	17 (100)	64 (81.0)	81 (84.4)	<i>P</i> = 0.065
Yes	0 (0)	15 (19.0)	15 (15.6)	
Enhancement				
Homogeneous	6 (35.3)	13 (16.5)	19 (19.8)	<i>P</i> < 0.001
Inhomogeneous	4 (23.5)	54 (68.4)	58 (60.4)	
Null	7 (41.2)	7 (8.9)	14 (14.6)	
Peripheric	0 (0)	5 (6.3)	5 (5.2)	
Intratumoral vascularization				
No	17 (100)	42 (53.2)	59 (61.5)	<i>P</i> < 0.001
Yes	0 (0)	37 (46.8)	37 (38.5)	
Vascular invasion				
No	17 (100)	66 (83.5)	83 (86.5)	<i>P</i> = 0.120
Yes	0 (0)	13 (16.5)	13 (13.5)	
Tissue invasion				
No	17 (100)	72 (91.1)	89 (92.7)	<i>P</i> = 0.350
Yes	0 (0)	7 (8.9)	7 (7.3)	

Appendix 1: Continued

MDCT feature	Thyroid mass		Total n (%) [*]	Significance
	Benign [n (%)] [*]	Malignant [n (%)] [*]		
Lymph node				
No	15 (88.2)	44 (55.7)	59 (61.5)	P = 0.013
Yes	2 (11.8)	35 (44.3)	37 (38.5)	
Distant metastasis				
No	17 (100)	75 (94.9)	92 (95.8)	P = 1.000
Yes	0 (0)	4 (5.1)	4 (4.2)	
Total	17 (17.7)	79 (82.3)	96 (100)	

^{*}Values between brackets are the relative percentage calculated within column.

Values in bold refer to statistically significant difference. For further explanations, see the text.

Appendix 2: The Table Resumes the MDCT Variables Assessed and the Possible Association with Incidental or Nonincidental Nature

MDCT feature	Thyroid mass		Total [n (%)] [*]	Significance [§]
	Incidental mass [n (%)] [*]	Nonincidental mass [n (%)] [*]		
Site				
Bilateral	4 (11.8)	14 (22.6)	18 (18.8)	P = 0.133
Right	11 (32.4)	26 (41.9)	37 (38.5)	
Left	19 (55.9)	22 (35.5)	41 (42.7)	
Shape				
Irregular	2 (5.9)	17 (27.4)	19 (19.8)	P = 0.04
Nodular	7 (20.6)	9 (14.5)	16 (16.7)	
Ovoid	25 (73.5)	36 (58.1)	61 (63.5)	
Appearance				
Homogeneous	15 (44.1)	13 (21.0)	28 (29.2)	P = 0.21
Inhomogeneous	19 (55.9)	49 (79.0)	68 (70.8)	
Mineralization				
No	31 (91.2)	50 (80.6)	81 (84.4)	P = 0.243
Yes	3 (8.8)	12 (19.4)	15 (15.6)	
Enhancement				
Homogeneous	7 (20.6)	12 (19.4)	19 (19.8)	P = 0.018
Inhomogeneous	16 (47.1)	42 (67.7)	58 (60.4)	
Null	10 (29.4)	4 (6.5)	14 (14.6)	
Peripheric	1 (2.9)	4 (6.5)	5 (5.2)	
Intratumoral vascularization				
No	28 (82.4)	31 (50.0)	59 (61.5)	P = 0.002
Yes	6 (17.6)	31 (50.0)	37 (38.5)	
Vascular invasion				
No	32 (94.1)	51 (82.3)	83 (86.5)	P = 0.129
Yes	2 (5.9)	11 (17.7)	13 (13.5)	
Tissue invasion				
No	33 (97.1)	56 (90.3)	89 (92.7)	P = 0.41
Yes	1 (2.9)	6 (9.7)	7 (7.3)	
Lymph node				
No	26 (76.5)	33 (53.2)	59 (61.5)	P = 0.030
Yes	8 (23.5)	29 (46.8)	37 (38.5)	
Distant metastasis				
No	34 (100)	58 (93.5)	92 (95.8)	P = 0.294
Yes	0 (0)	4 (6.5)	4 (4.2)	
Total	34 (35.4) ²	62 (64.6) ²	96 (100)	

^{*}Values between brackets are the relative percentage calculated within column.

[§]Values in bold refer to statistically significant difference. For further explanations, see the text.

REFERENCES

1. Barber LG. Thyroid tumors in dogs and cats. *Vet Clin North Am Small Anim Pract* 2007;37:756–773.
2. Wucherer KL, Wilke V. Thyroid cancer in dogs: an update based on 638 cases (1995–2005). *J Am Anim Hosp Assoc* 2010;46:249–254.
3. Taeymans O, Peremans K, Saunders JH. Thyroid imaging in the dog: current status and future directions. *J Vet Intern Med* 2007;21:673–84.
4. Feeney DA, Anderson KL. Nuclear imaging and radiation therapy in canine and feline thyroid disease. *Vet Clin North Am Small Anim Pract* 2007;37:799–821.
5. Taeymans O, Dennis R, Saunders JH. Magnetic resonance imaging of the normal canine thyroid gland. *Vet Radiol Ultrasound* 2008;49:238–242.
6. Taeymans O, Schwarz T, Duchateau L, et al. Computed tomographic features of the normal canine thyroid gland. *Vet Radiol Ultrasound* 2008;49:13–19.
7. Mattoon JS, Nyland TG. Ultrasound-guided aspiration and biopsy procedures. In: *Small animal diagnostic ultrasound*, 3rd ed. St. Louis, MO: Elsevier Saunders, 2014;60.
8. Taeymans O, Penninck DG, Peters RM. Comparison between clinical, ultrasound, CT, MRI, and pathology findings in dogs presented for suspected thyroid carcinoma. *Vet Radiol Ultrasound* 2013;54:61–70.
9. Deitz K, Gilmour L, Wilke V, Riedesel E. Computed tomographic appearance of canine thyroid tumours. *J Small Anim Pract* 2014;55:323–329.
10. Mevawalla N, McMullen T, Sidhu S, Sywak M, Robinson B, Delbridge L. Presentation of clinically solitary thyroid nodules in surgical patients. *Thyroid* 2011;21:55–59.
11. Bertolini G, Marcon O, Borsetto A, Finesso S, Caldin M. Computed tomography of incidental and nonincidental thyroid lesions in dogs. Abstracts of papers presented at the 16th congress of the International Veterinary Radiology Association and the annual meeting of the European Association and College of Veterinary Diagnostic Imaging, Bursa, Turkey. *Vet. Radiol Ultrasound* 2013;54:415.
12. Pollard RE, Bohannon LK, Feldman EC. Prevalence of incidental thyroid nodules in ultrasound studies of dogs with hypercalcemia (2008–2013). *Vet Radiol Ultrasound* 2015;56:63–67.
13. Schultz RM, Wisner ER, Johnson EG, MacLeod JS. Contrast-enhanced computed tomography as a preoperative indicator of vascular invasion from adrenal masses in dogs. *Vet Radiol Ultrasound* 2009;50:625–629.
14. Nguyen SM, Thamm DH, Vail DM, London CA. Response evaluation criteria for solid tumours in dogs (v1.0): a Veterinary Cooperative Oncology Group (VCOG) consensus document. *Vet Comp Oncol* 2015;13:176–83.
15. Liptak JM. Canine thyroid carcinoma. *Clin Tech Small Anim Pract* 2007;22:75–81.
16. Handa U, Garg S, Mohan H, Nagarkar N. Role of fine needle aspiration cytology in diagnosis and management of thyroid lesions: a study on 434 patients. *J Cytol* 2008;25:13–17.
17. Harari J, Patterson JS, Rosenthal RC. Clinical and pathologic features of thyroid tumors in 26 dogs. *J Am Vet Med Assoc* 1986;188:1160–1164.
18. Thompson EJ, Stirtzinger T, Lumsden JH, et al. Fine needle aspiration cytology in the diagnosis of canine thyroid carcinoma. *Can Vet J* 1980;21:186–188.
19. Ménard M, Fontaine M, Morin M. Fine needle aspiration biopsy of malignant tumors in dogs and cats: a report of 102 cases. *Can Vet J* 1986;27:504–10.